An aerial photograph capturing a massive tsunami wave crashing over a coastal town. The water is dark and turbulent, towering over buildings and streets. A blue sign with the word 'MIYAKO' is visible on a street. The scene is chaotic, with debris and dust kicked up by the force of the water.

# Uncovering the Mysteries of Tsunami Generation and Anomalous Seismic Radiation in the Shallow Subduction Zone

*Shuo Ma<sup>1</sup> and Evan Hirakawa<sup>1,2</sup>*

<sup>1</sup>Department of Geological Sciences  
San Diego State University

<sup>2</sup>Scripps Institution of Oceanography  
University of California, San Diego

*Rupture Dynamics Code Validation Workshop  
March 15, 2013*

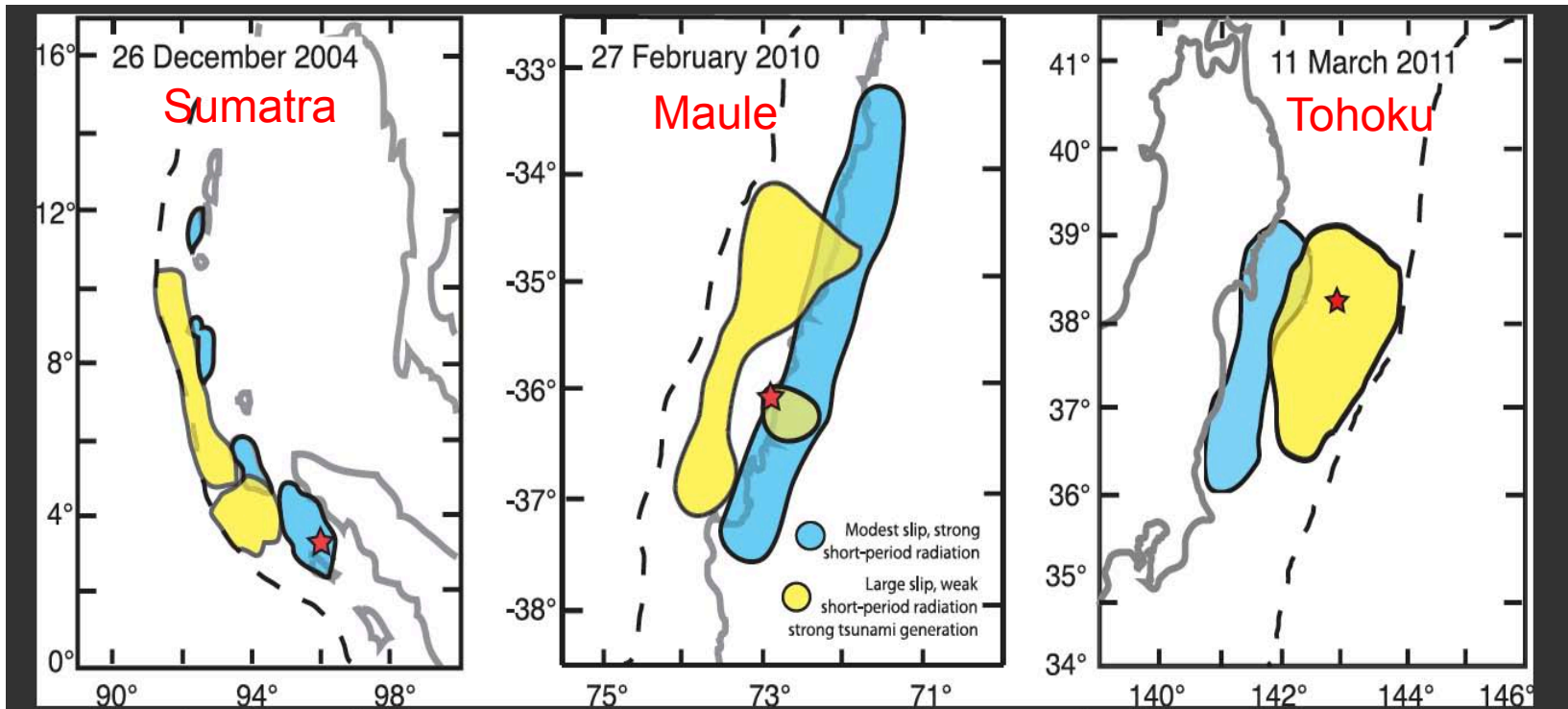
# 40-Year Puzzles About Tsunami Earthquakes

Identified by Hiroo Kanamori in 1972

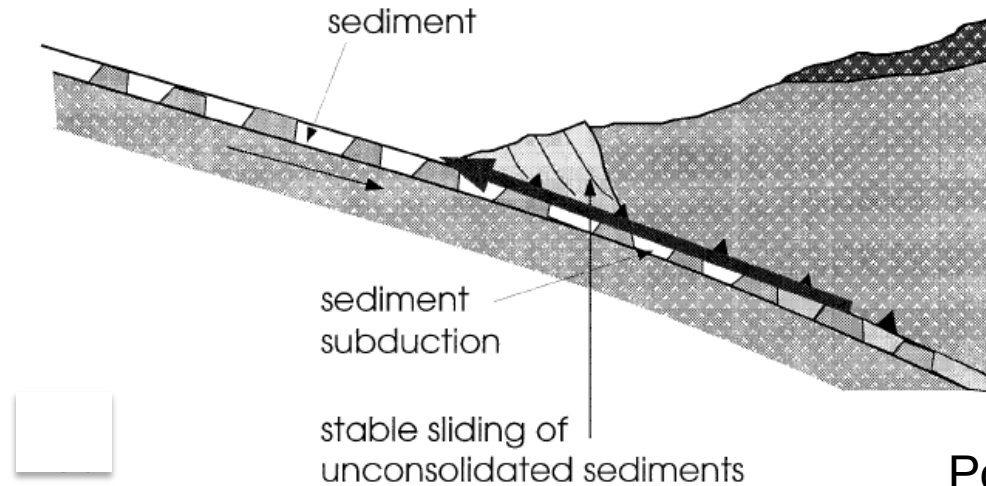
- Large tsunamis
- Depletion in high-frequency radiation
- Slow rupture velocity and long rupture duration
- Possibly small stress drop and slip velocity
- Low energy-to-moment ratio
- Occur in a frictionally stable (velocity-strengthening) or conditionally stable regime

# Characteristics of Large Tsunamigenic Earthquakes

- Weak high-frequency radiation
- Slow rupture velocity (long rupture duration)
- Strong tsunami generation



# Mechanism for Slow Rupture Propagation: Sediments and Fault Morphology



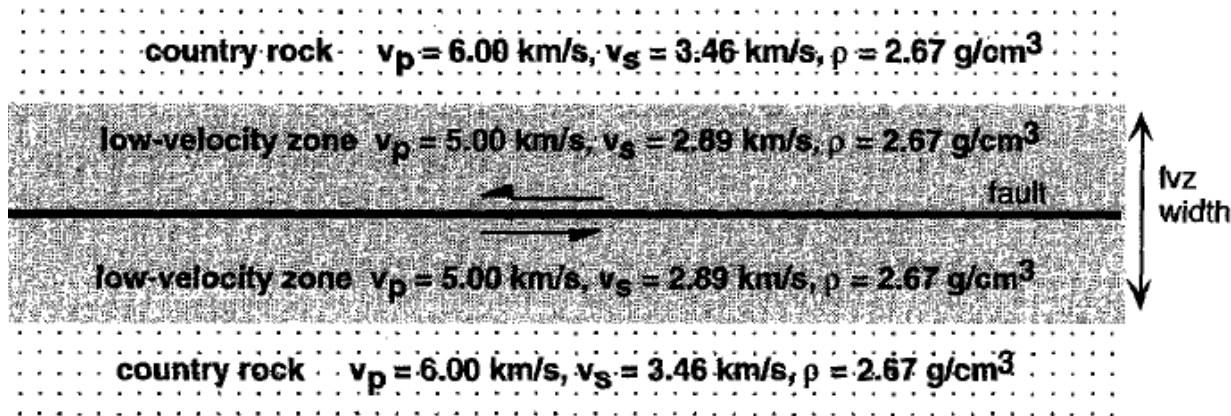
Polet and Kanmori (2000)

- Presence of sediments gives rise to slow rupture velocity.
- Horst-and-graben structure on the plate interface allows the rupture to reach the trench.
- Fault roughness causes large fracture energy.

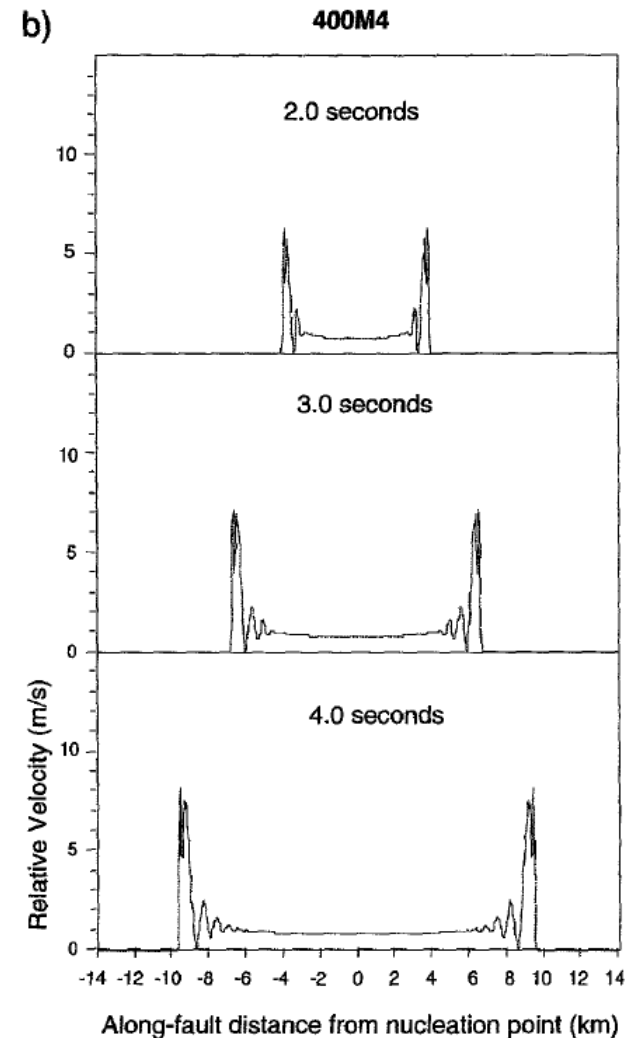
One inconsistency:

Fault roughness tends to generate more high-frequency radiation.

# Dynamic Rupture Simulations in a Low-Velocity Fault Zone



Harris and Day (1997)



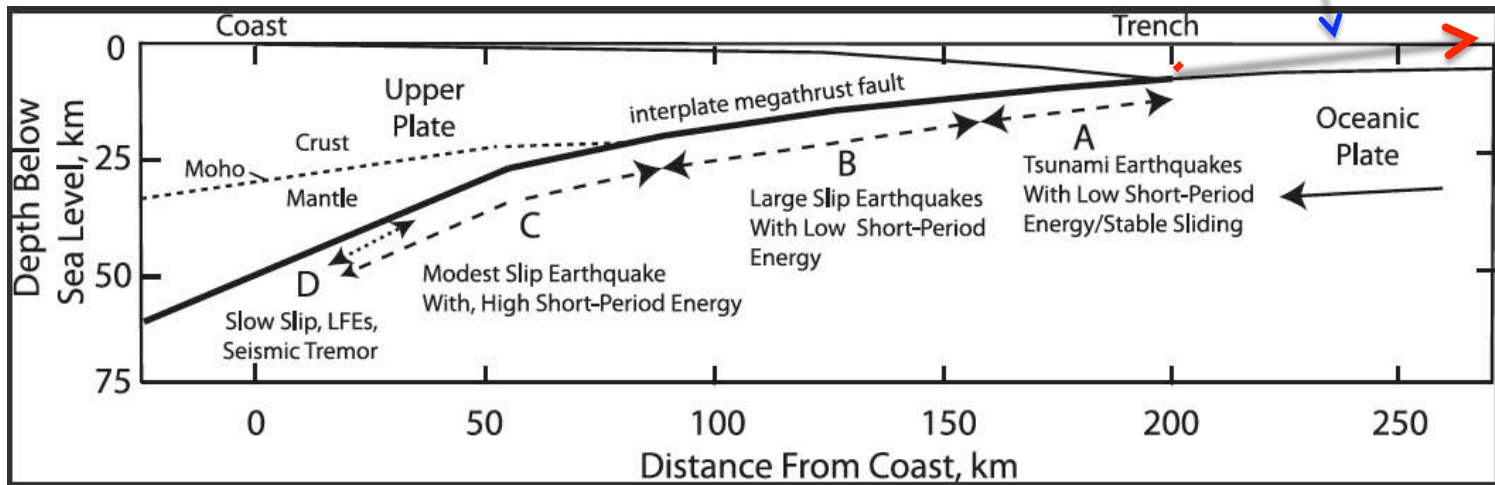
## Sediments in the fault zone:

- Promote pulse-like rupture.
- Do not always decrease rupture velocity, and can instead lead to supershear rupture.

More high-frequency radiation!

# Mechanism for Tsunami Generation: Large Shallow Slip

Nearly horizontal displacement  
Inefficient to generate tsunami



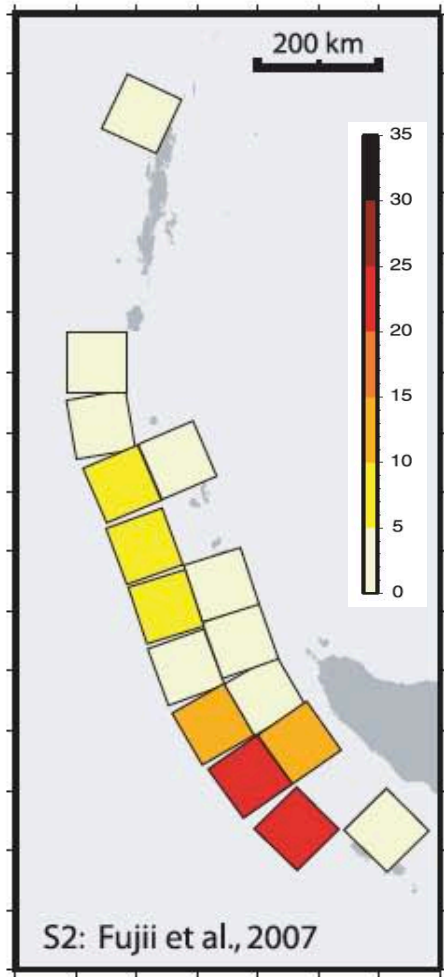
Lay et al. (2012)

$$\text{uplift} \approx \text{slip} \times \sin(\text{dip})$$

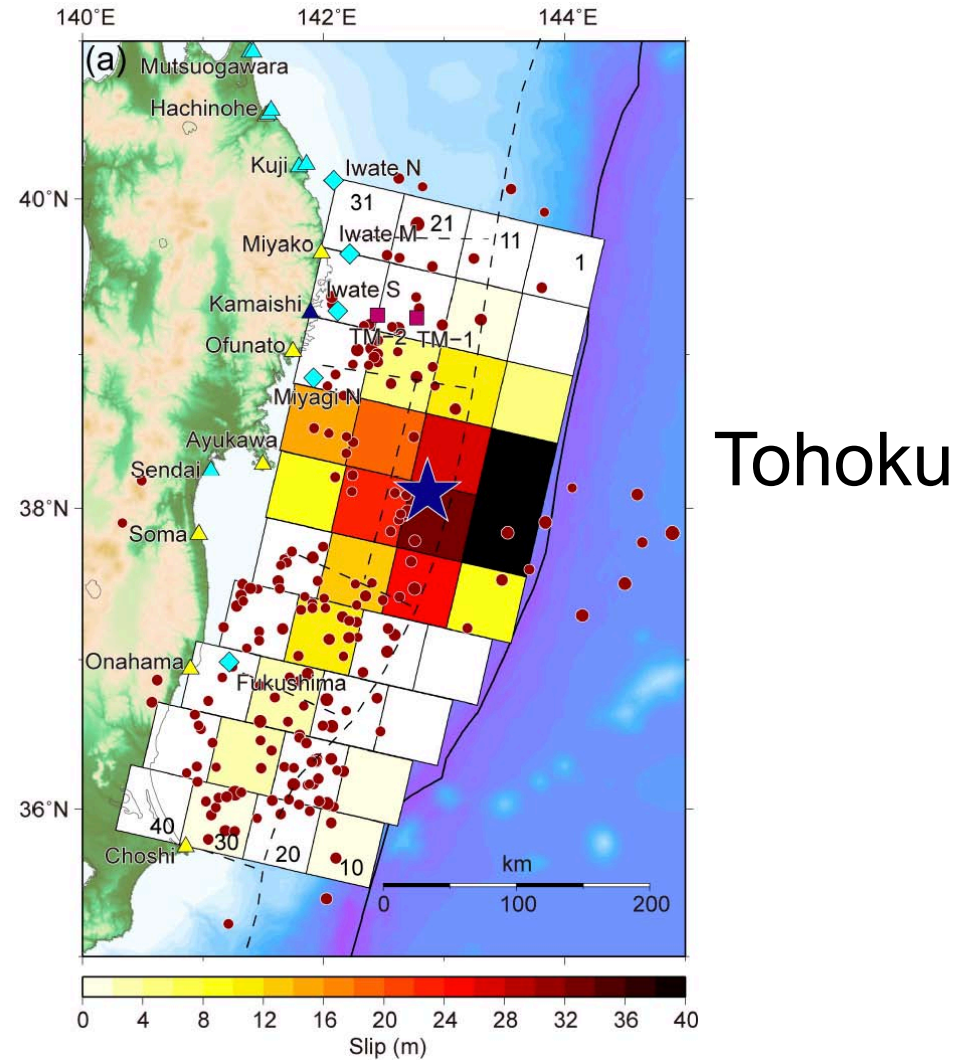
Shallow fault dip · **?** → large slip

# Slip Models Using Tsunami Data

Sumatra

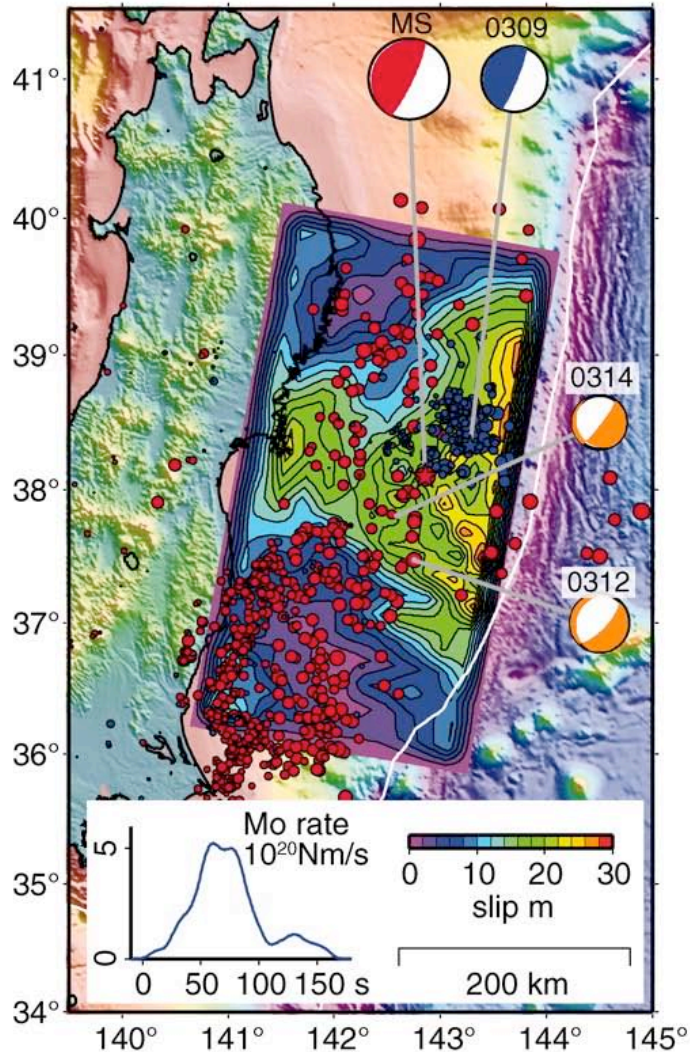


Fujii et al. (2007)

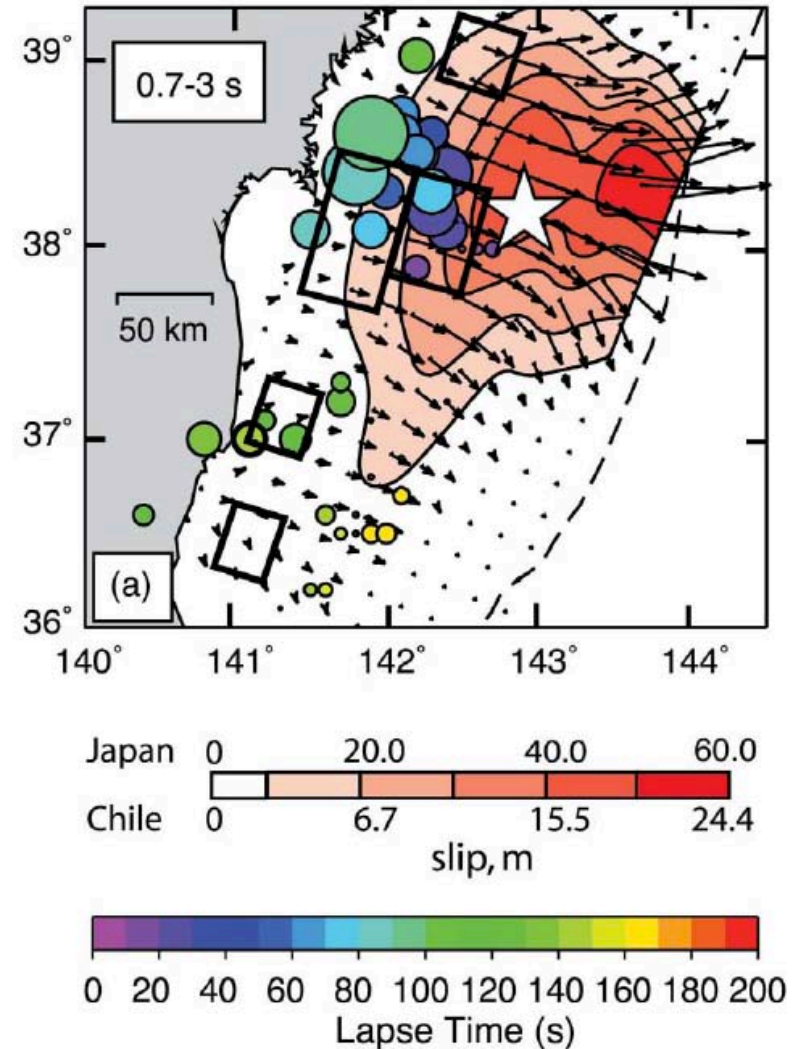


Fujii et al. (2011)

# Tohoku Slip Models Using Teleseismic or GPS Data



Ide et al. (2011)

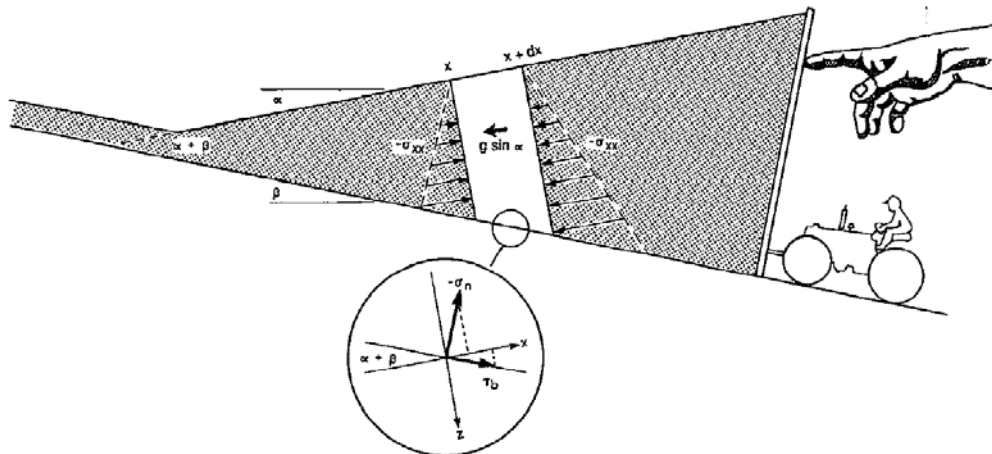


Lay et al. (2012)

# Critical Taper (Coulomb Wedge) Theory

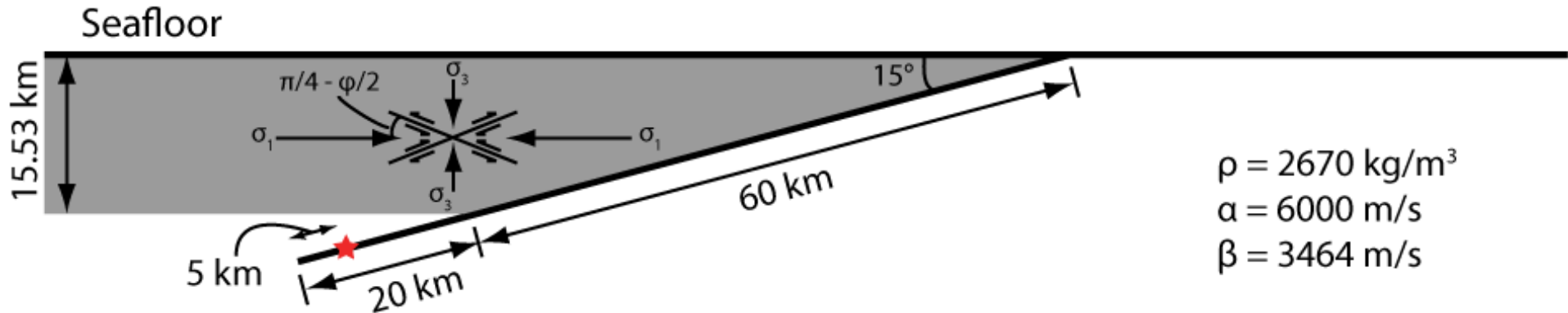


“The overall mechanics of fold-and-thrust belts and accretionary wedges along compressive plate boundaries is considered to be **analogous to that of a wedge of soil or snow in front of a moving bulldozer**... The critical taper is the shape for which the wedge is **on the verge of failure** under horizontal compression **everywhere, including the basal décollement.**”



Davis et al. (1983)

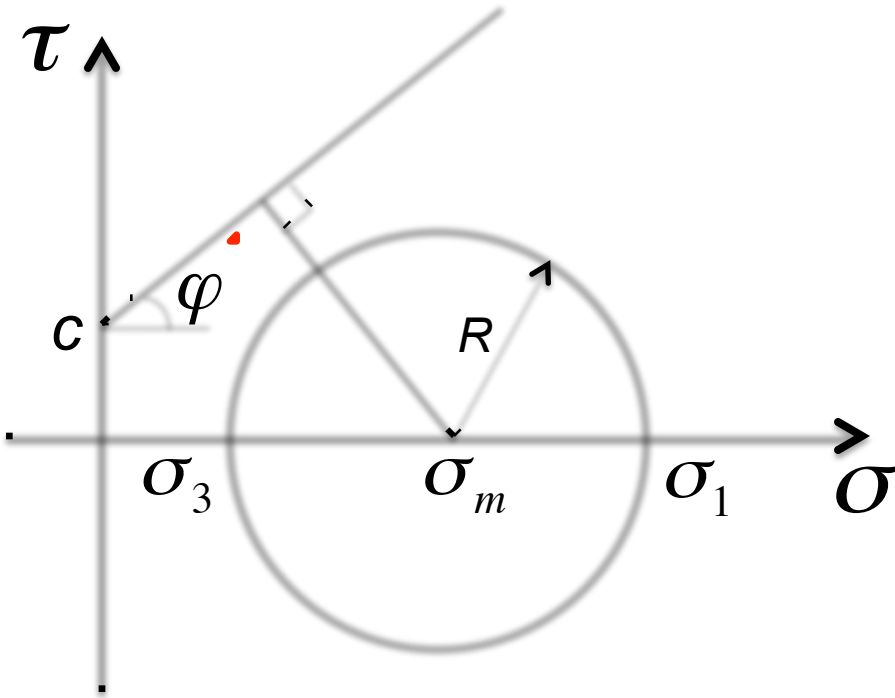
# Fault Geometry and Stress Conditions



Depth-dependent effective stresses:

$$\begin{aligned} \sigma_3 = \sigma_{zz} &= -(1 - \lambda) \rho g z \\ \sigma_1 = \sigma_{xx} &= 3.7469 \sigma_{zz} \end{aligned} \quad \rightarrow \mu_0 = \tau / \sigma_N = 0.58$$

# Mohr-Coulomb Failure Criterion



Closeness-to-Failure ( $CF$ )

$$CF = \frac{R}{c \cos \varphi - \sigma_m \sin \varphi}$$

$$c = 0.017 \sigma_{zz}$$

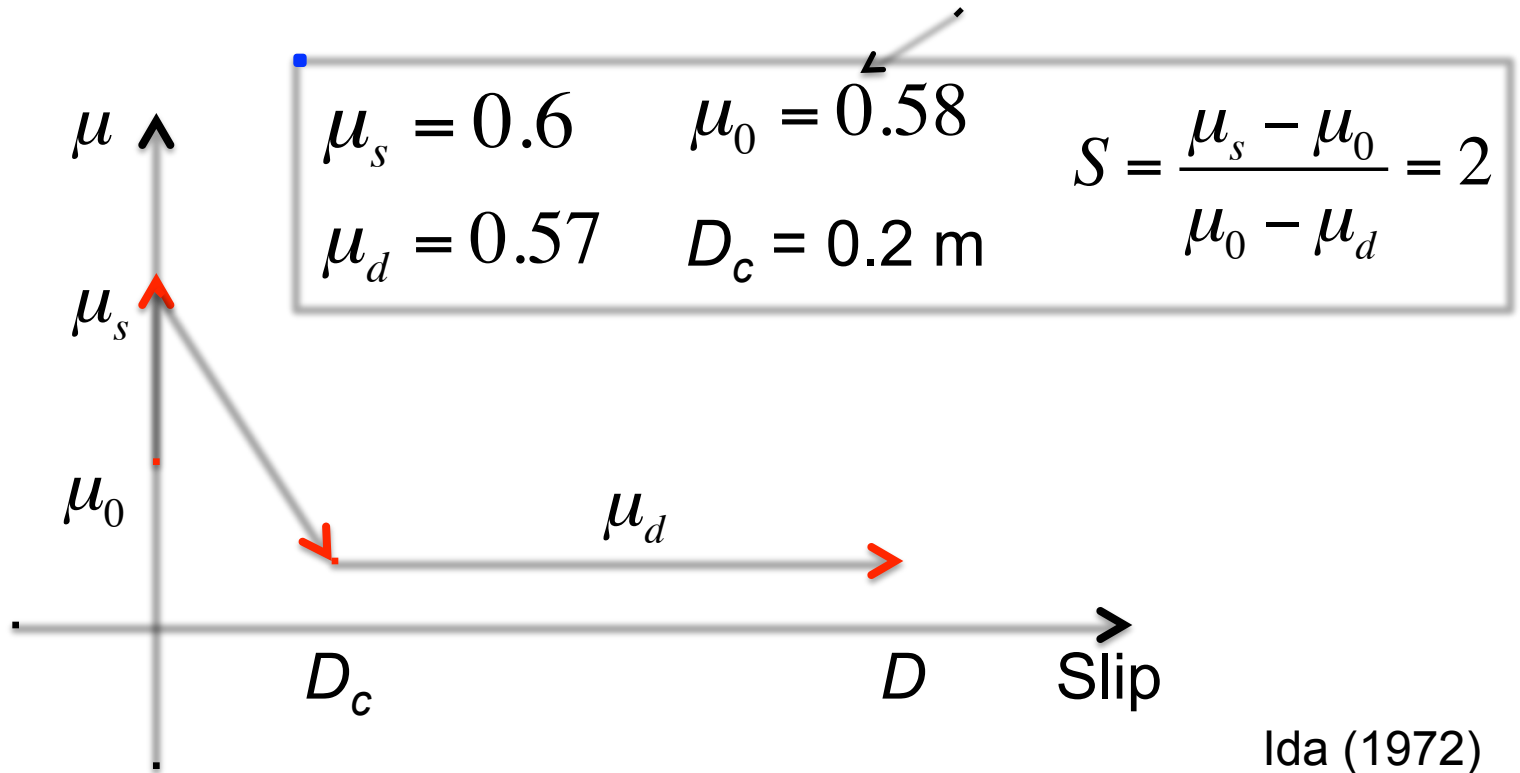
$$\tan \varphi = 0.7095$$

$$CF = 0.99$$

Sub-critical wedge

# Slip-Weakening Friction

The fault is also close to failure.



No velocity-strengthening friction is used.

# Pore Pressure Change in Undrained Condition

$$\Delta p = B \frac{1 + \nu_u}{3} (\Delta \sigma_{xx} + \Delta \sigma_{zz})$$

$B$ : Skempton's coefficient

$\nu_u$ : undrained Poisson's ratio

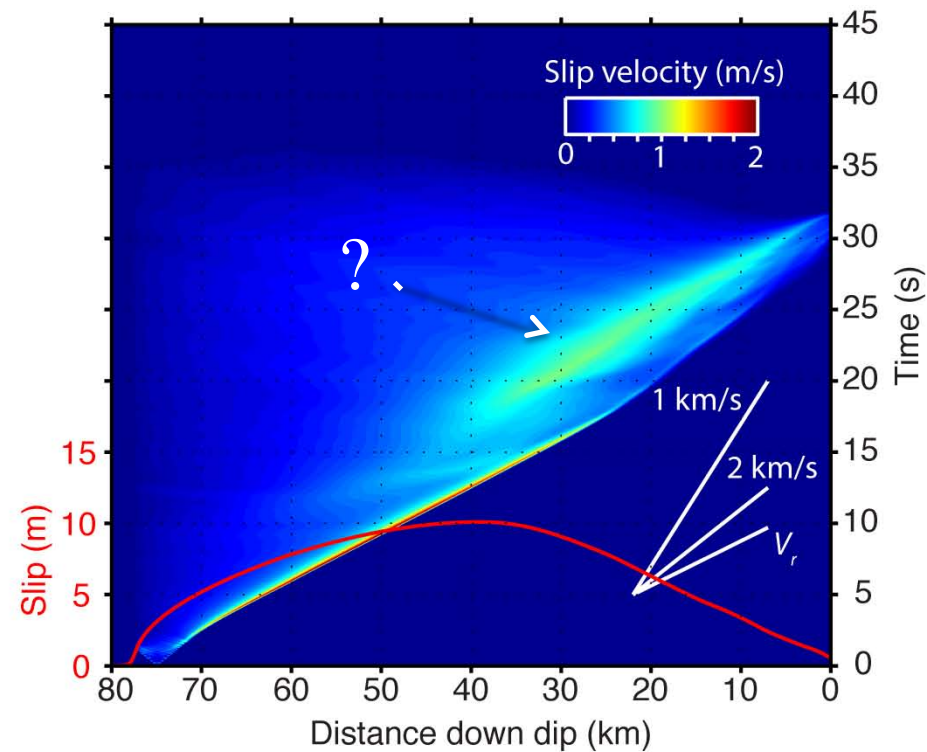
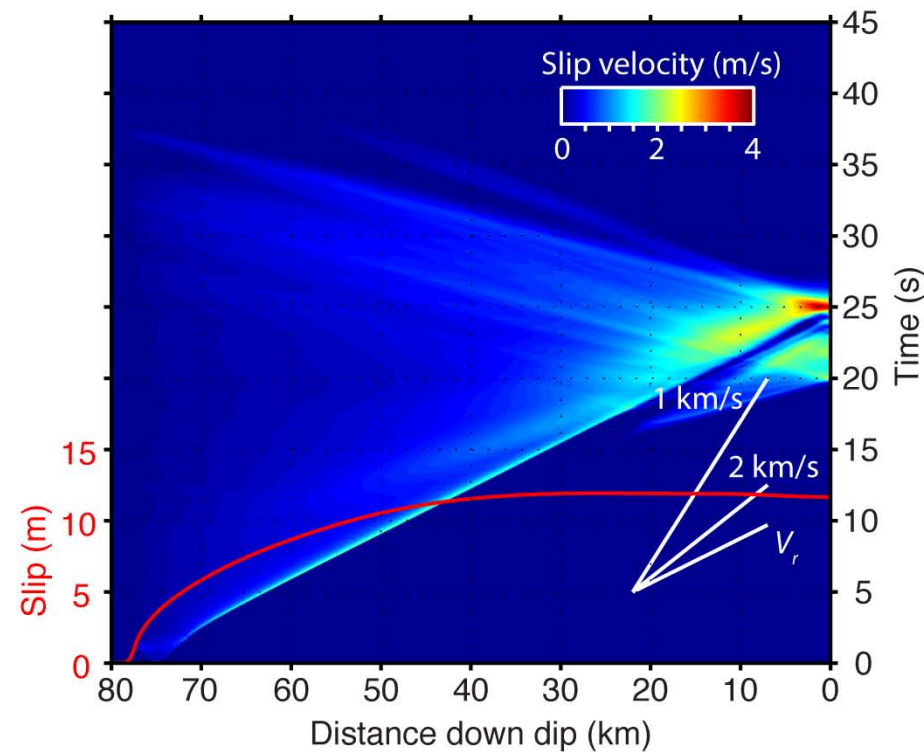
We use  $B = 0.3$  everywhere in the wedge.

# Rupture Movie (Hydrostatic)

# Time-Distance Plots of Slip Velocity and Slip Distribution (Red)

## Elastic

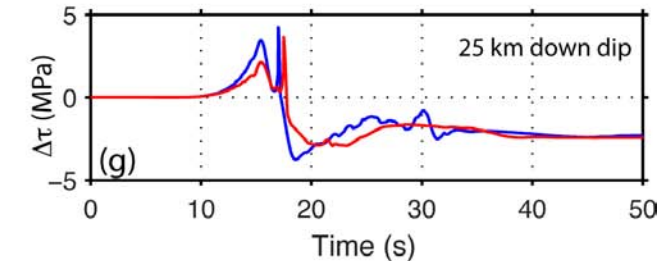
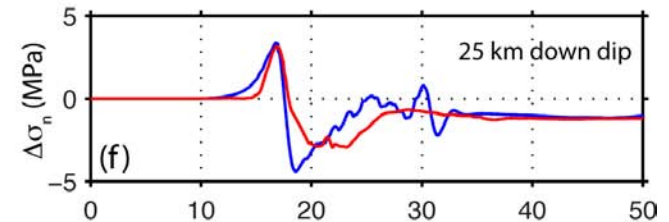
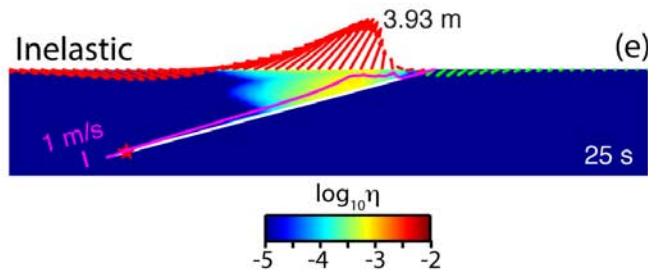
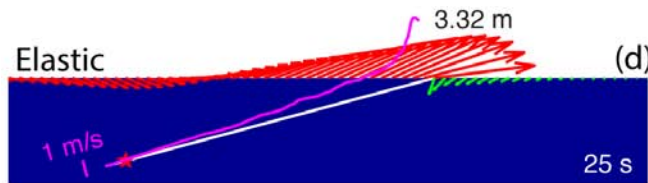
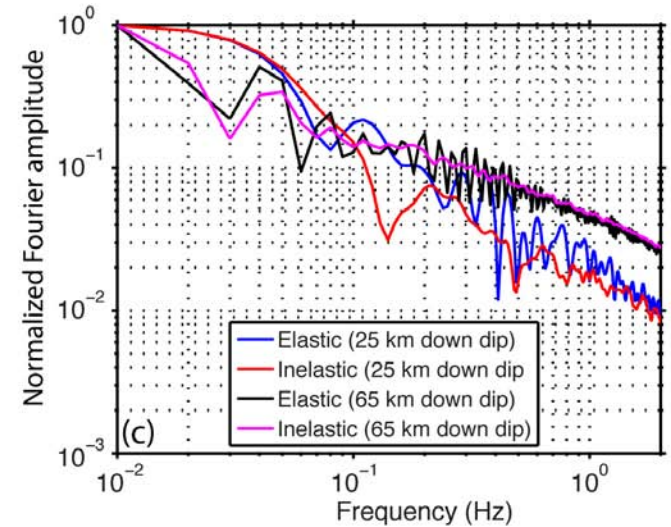
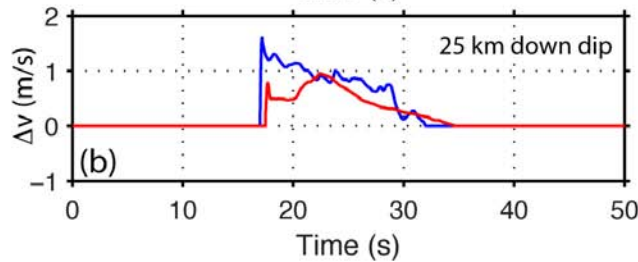
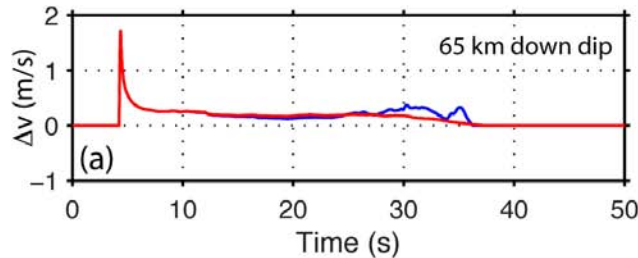
## Inelastic



Large rupture velocity  
Large slip near the trench

Slow rupture velocity  
Small slip near the trench

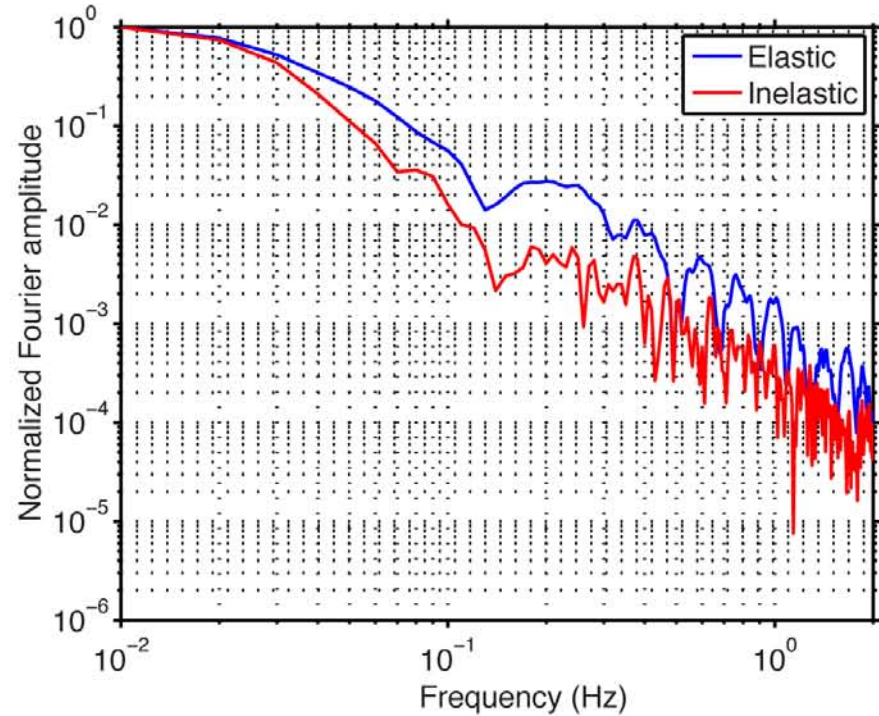
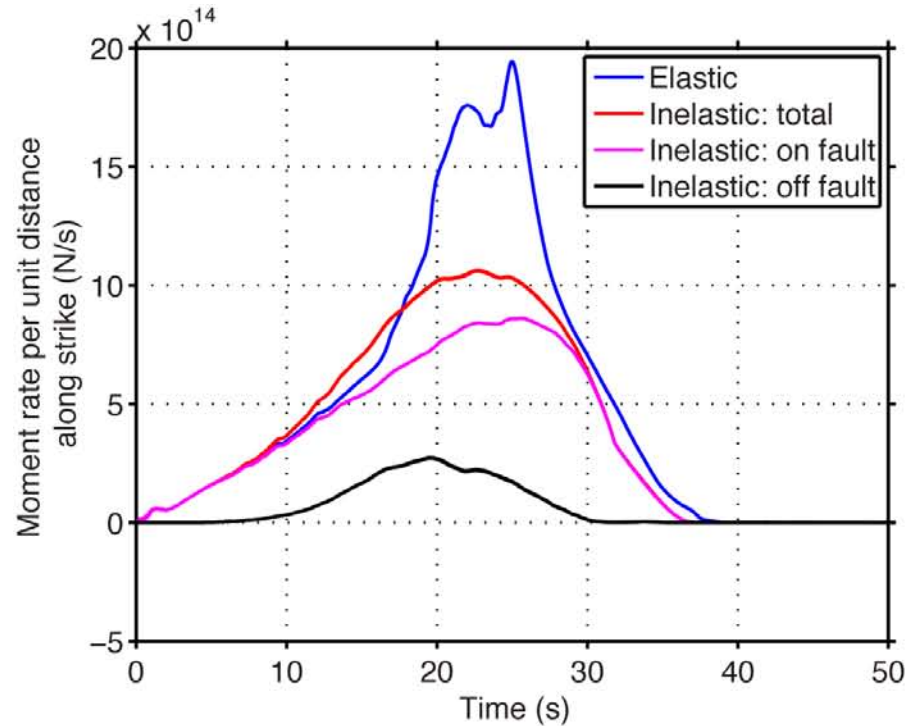
# Time Histories at 25 km and 65 km Down Dip



- More gradual stress change
- Smoother slip velocity
- Less high-frequency radiation

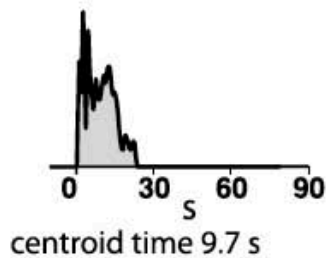


# Moment Rate Time Functions and Spectra

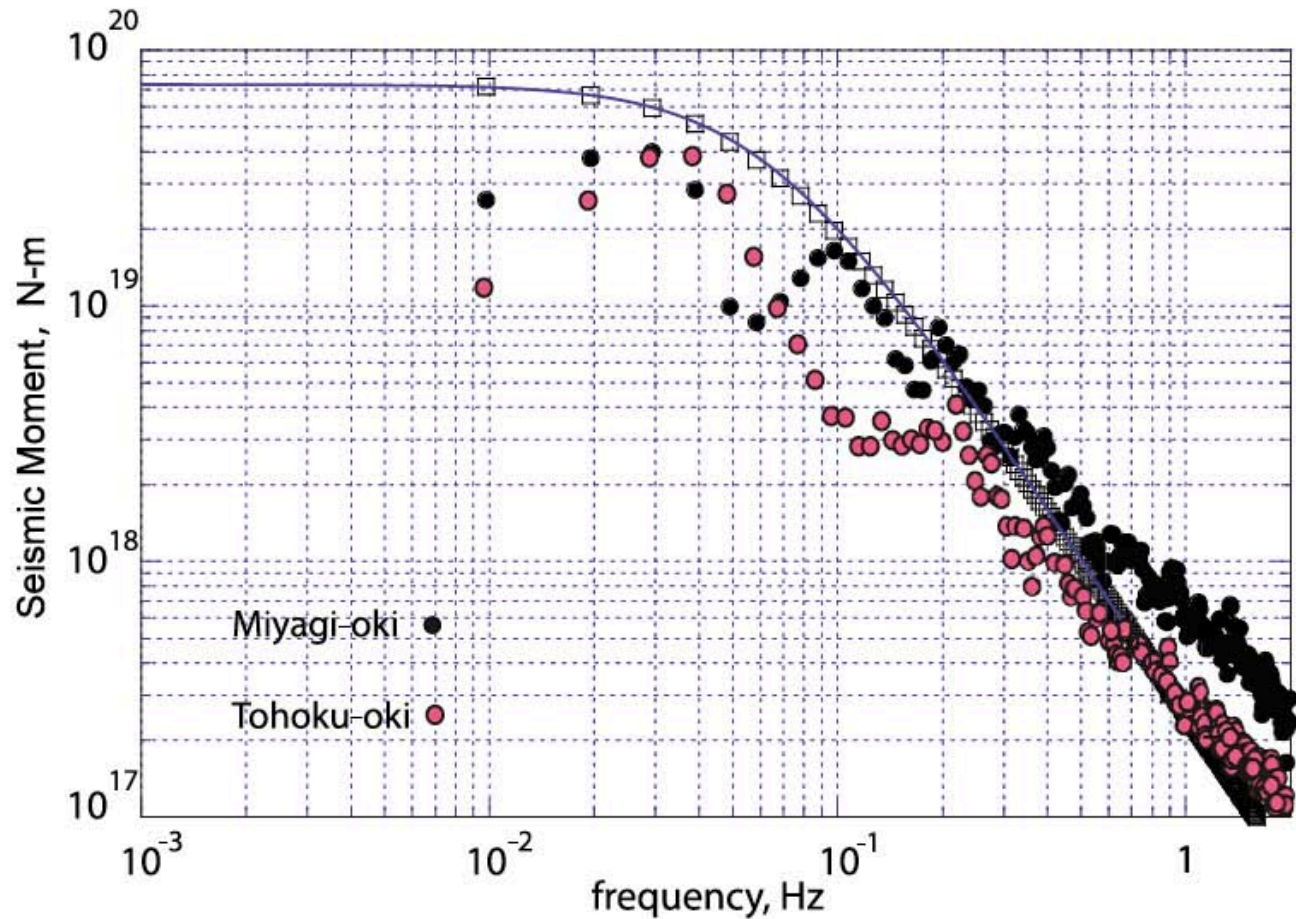
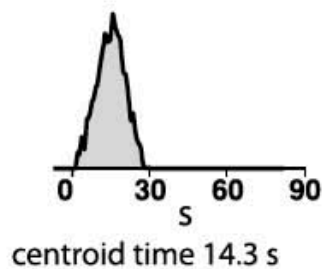


**Less high-frequency radiation!**

16 August 2005 Miyagi-oki  
 $M_0 = 0.9 \times 10^{20}$  Nm ( $M_w = 7.2$ )  
Depth 36 km



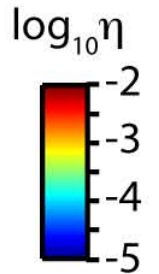
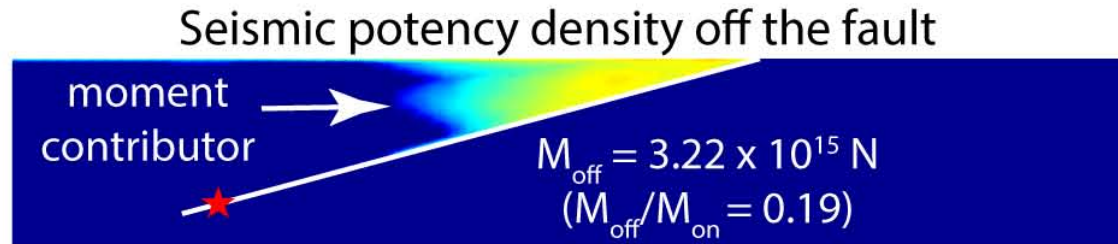
9 March 2011 Tohoku-oki  
 $M_0 = 1.9 \times 10^{20}$  Nm ( $M_w = 7.5$ )  
Depth 14 km



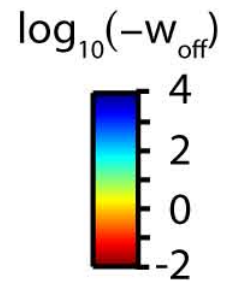
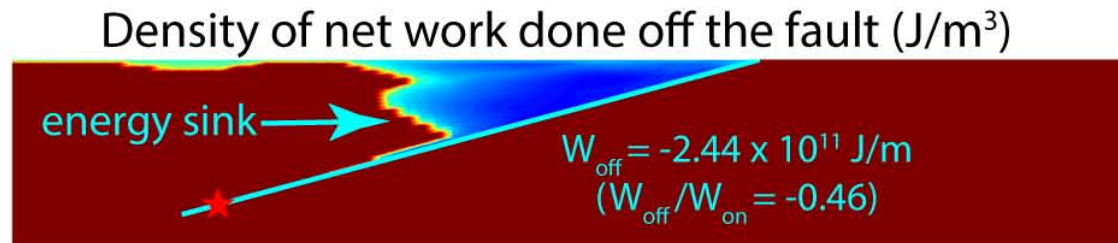
Lay et al. (2012)

# Moment-Scaled Radiated Energy

moment contributor



energy sink

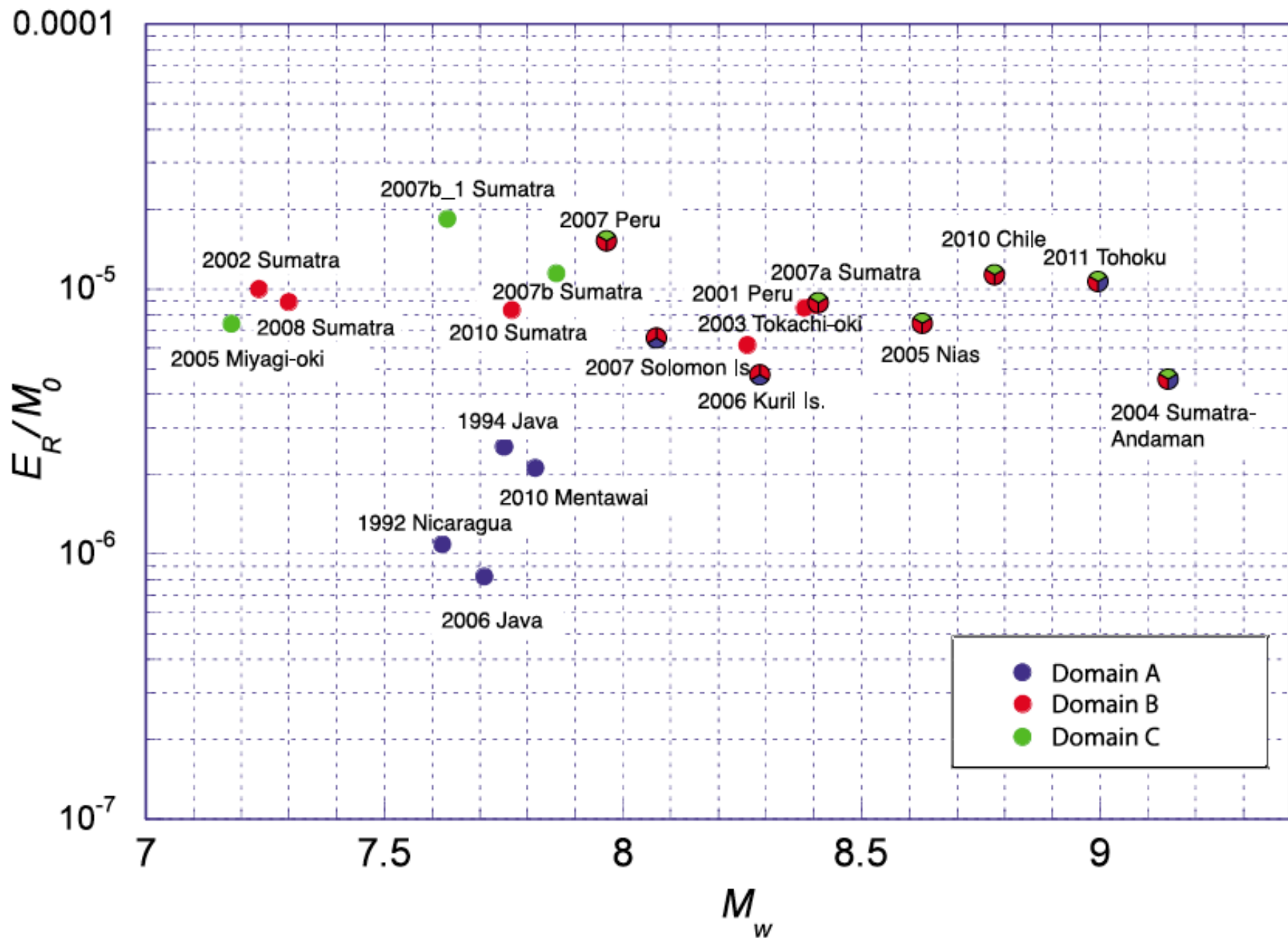


Elastic

$M: 2.52 \times 10^{16} \text{ N}$   
 $E^R: 6.12 \times 10^{11} \text{ J/m}$   
 $E^R/M: 2.43 \times 10^{-5}$

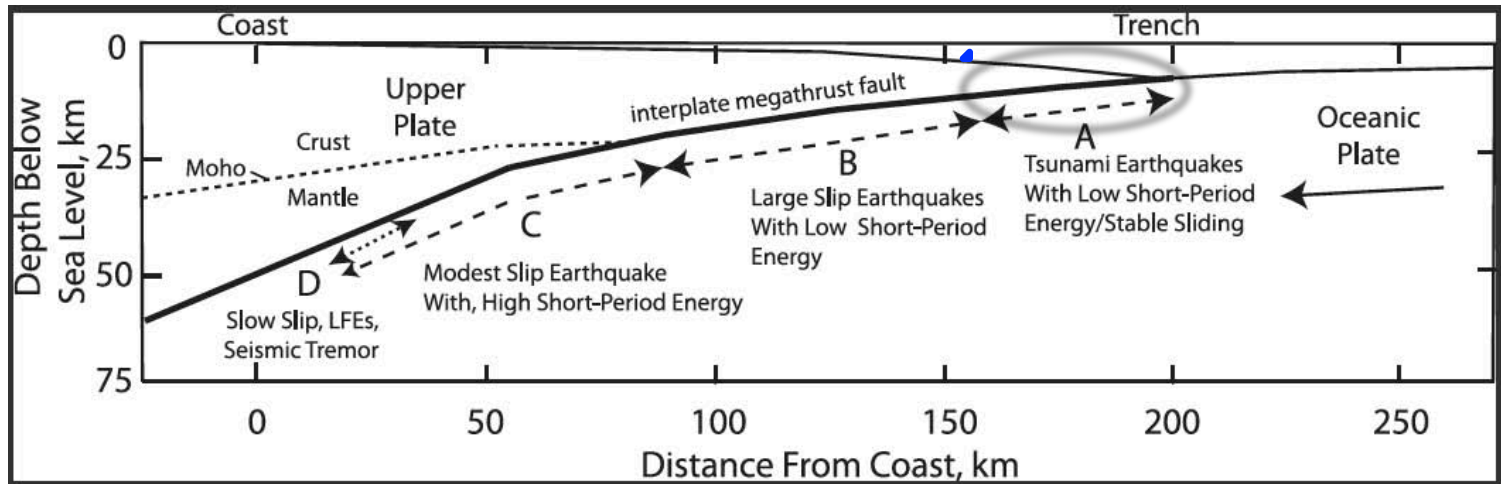
Inelastic

$M: 1.99 \times 10^{16} \text{ N}$   
 $E^R: 2.91 \times 10^{11} \text{ J/m}$   
 $E^R/M: 1.46 \times 10^{-5}$



# Another Look at Subduction Zone Fault Geometry

Large seafloor uplift



Shallower fault dip

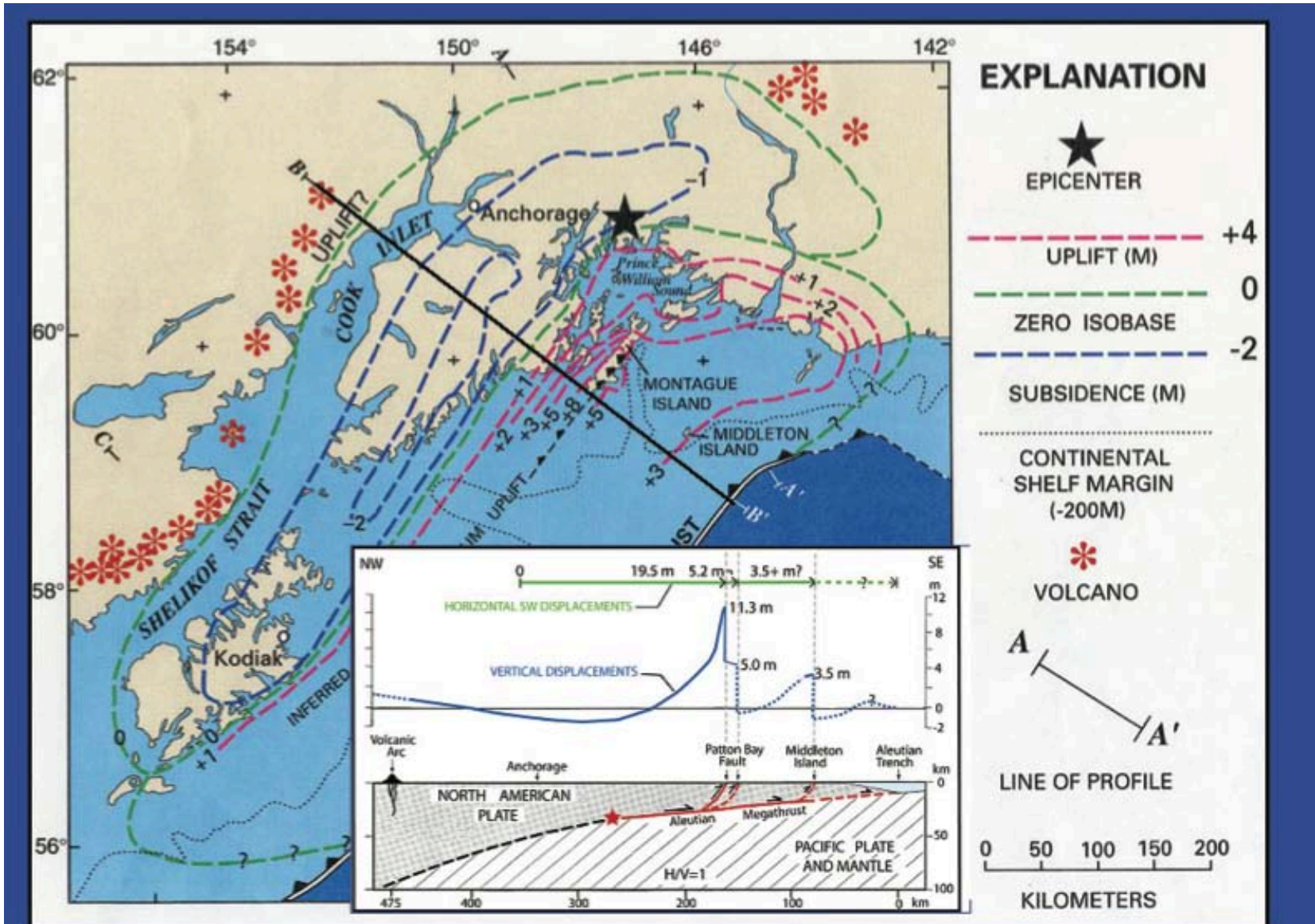
Smaller confining pressure

Easier to fail

Larger seafloor uplift

Less high-frequency radiation

# Coseismic Displacements for the 1964 Alaska Earthquake



# Conclusions

Extensive Coulomb failure in the wedge provides **a unifying interpretation** to nearly all anomalous features of shallow subduction earthquakes, including:

- Slow rupture velocity
- Efficient tsunami generation
- Deficiency in high-frequency radiation
- Low energy-to-moment ratio



Namazus